Biochemistry 1987, 26, 6531-6538

NMR Analyses of the Conformations of L-Isoleucine and L-Valine Bound to *Escherichia coli* Isoleucyl-tRNA Synthetase[†]

Daisuke Kohda,[‡,§] Gota Kawai,[‡] Shigeyuki Yokoyama,*[,‡] Makoto Kawakami,[∥] Shoji Mizushima,[⊥] and Tatsuo Miyazawa[‡]

Department of Biophysics and Biochemistry, Faculty of Science, University of Tokyo, Hongo, Bunkyo-ku, Tokyo 113, Japan, and Institute of Molecular Biology, Faculty of Science, and Laboratory of Microbiology, School of Agriculture, Nagoya University, Chikusa-ku, Nagoya 464, Japan

Received September 10, 1986; Revised Manuscript Received April 10, 1987

ABSTRACT: The 400-MHz ^{1}H NMR spectra of L-isoleucine and L-valine were measured in the presence of *Escherichia coli* isoleucyl-tRNA synthetase (IleRS). Because of chemical exchange of L-isoleucine or L-valine between the free state and the IleRS-bound state, a transferred nuclear Overhauser effect (TRNOE) was observed among proton resonances of L-isoleucine or L-valine. However, in the presence of isoleucyl adenylate tightly bound to the amino acid activation site of IleRS, no TRNOE for L-isoleucine or L-valine was observed. This indicates that the observed TRNOE is due to the interaction of L-isoleucine or L-valine with the amino acid activation site of IleRS. The conformations of these amino acids in the amino acid activation site of IleRS were determined by the analyses of time dependences of TRNOEs and TRNOE action spectra. The IleRS-bound L-isoleucine takes the gauche$^+$ form about the C_α–C_β bond and the trans form about the C_β–$C_{\gamma1}$ bond. The IleRS-bound L-valine takes the gauche$^-$ form about the C_α–C_β bond. Thus, the conformation of IleRS-bound L-valine is the same as that of IleRS-bound L-isoleucine except for the δ-methyl group. The side chain of L-isoleucine or L-valine lies in an aliphatic hydrophobic pocket of the active site of IleRS. Such hydrophobic interaction with IleRS is more significant for L-isoleucine than for L-valine. The TRNOE analysis is useful for studying the amino acid discrimination mechanism of aminoacyl-tRNA synthetases.

The fidelity in the translation of genetic information from the nucleotide sequences to amino acid sequences is due to the strict specificities of aminoacyl-tRNA synthetases for cognate amino acid and tRNA species. Isoleucyl-tRNA synthetase (IleRS)[1] discriminates between L-isoleucine and L-valine with a very low error rate in protein biosynthesis (Loftfield & Vanderjagt, 1972). The rate of formation of valyl adenylate is only about $^1/_{100}$th time as that of isoleucyl adenylate (Loftfield & Eigner, 1966). The structure of the amino acid activation site of IleRS has been studied by using a variety of isoleucine analogues (Holler et al., 1973; Flossdorf et al., 1976). Further, IleRS has been suggested to have the proofreading activity for the hydrolysis of valyl adenylate incorrectly formed (Fersht, 1977; Hopfield et al., 1976). Thus, IleRS is one of the best characterized aminoacyl-tRNA synthetases with regard to the amino acid discrimination. In relation to these data, the conformation analyses of amino acids bound in the active site of IleRS will be important for understanding the discrimination mechanism of IleRS at the molecular level.

In the hope of elucidating the conformations of amino acids as bound to IleRS, in the present study, we have used the method of transferred nuclear Overhauser effect (TRNOE). The TRNOE method is useful for studying the conformations of small flexible molecules bound to macromolecules and has been applied for the conformation studies on a ligand bound to dihydrofolate reductase (Cayley et al., 1979), nucleotides bound to proteins (Gronenborn & Clore, 1982, 1984; Gronenborn et al., 1984a; Banerjee et al., 1985; Machida et al., 1985; Ferrin & Mildvan, 1985), trinucleotides bound to tRNA species (Gronenborn et al., 1984b; Clore et al., 1984), and furthermore on peptides bound to a perdeuteriated phospholipid bilayer (Wakamatsu et al., 1983, 1986a,b, 1987). In the present study, we have succeeded, by the TRNOE method, in elucidating the conformations of L-isoleucine and L-valine as bound to the amino acid activation site of IleRS.

EXPERIMENTAL PROCEDURES

Escherichia coli IleRS was purified from *E. coli* cells harboring the *ileS* gene on a runaway-replication plasmid (Kawakami et al., 1985) and was stored at −80 °C in 0.15 M potassium phosphate (pH 7.0) containing 1 mM dithiothreitol and 25% glycerol. L-Isoleucine and L-valine were purchased from Wako Pure Chemical Industries (Tokyo), and 2-(*p*-toluidino)naphthalene-6-sulfonate (TNS) was from Nakarai Chemicals (Tokyo). ATP was obtained from Sigma, and the concentration of ATP·Mg in stock solution was determined from the molar extinction coefficient of ATP (ϵ_{259} = 15 400 cm^{-1} M^{-1}). ^2H_2O (99.85%) was purchased from the Commissariat â l'Energie Atomique.

Fluorescence Measurements. The fluorescence of TNS was measured with a Hitachi F-4000 fluorescence spectrometer, where the cell temperature was controlled at 37 °C. The

---

[†] This work was supported in part by Grant-in-Aid for Distinguished Research 60060004 and by Grants-in-Aid for Scientific Research 56470126 and 59780166 from the Ministry of Education, Science and Culture of Japan.

[‡] University of Tokyo.

[§] Present address: Department of Medical Chemistry, Tokyo Metropolitan Institute of Medical Science, Honkomagome, Bunkyo-ku, Tokyo 113, Japan.

[∥] Faculty of Science, Nagoya University.

[⊥] School of Agriculture, Nagoya University.

[1] Abbreviations: IleRS, isoleucyl-tRNA synthetase; TNS, 2-(*p*-toluidino)naphthalene-6-sulfonate; TRNOE, transferred nuclear Overhauser effect; kDa, kilodalton(s).

0006-2960/87/0426-6531$01.50/0

sample solution contained 10 mM potassium phosphate (pH 7.0), 5 mM 2-mercaptoethanol, and 50 mM KCl, in addition to 0.2 μM IleRS, 20 μM TNS, and varying concentrations of L-isoleucine or L-valine. The fluorescence was excited at 366 nm and observed at 470 nm, and the dissociation constant of the complex of IleRS and amino acid was determined by the analysis of the fluorescence intensity of TNS as a function of amino acid concentration (Holler et al., 1971).

NMR Measurements. The ^2H_2O solution of IleRS for proton NMR measurements was prepared by repeated ultrafiltration with a Centricon-30 (Amicon; M_r 30 000 cutoff), thus avoiding possible denaturation during lyophilization. The membrane was thoroughly washed, in advance, with distilled H_2O. One milliliter of H_2O solution containing 10 mg of IleRS was concentrated to about 0.1 mL by the use of a Centricon unit (2 mL). To this concentrated solution was added 1 mL of buffered ^2H_2O containing 10 mM potassium phosphate (pH 7.0)[2] and 50 mM KCl. The solution (1.1 mL) was concentrated again to about 0.1 mL. This process was repeated 5 times in order to prepare a ^2H_2O solution of native IleRS. The final volume of sample solution was adjusted to 0.35 mL for NMR measurements. The concentration of IleRS was determined by using the molecular mass (115 kDa) (Kawakami et al., 1985) and the specific absorbance (A_{280} = 1.5m $\text{cm}^{-1}\cdot\text{mg}^{-1}\cdot\text{mL}$ by the dry weight method). The final concentration of IleRS was 0.3 mM. The mole ratio of L-isoleucine/IleRS was 16 while the ratio of L-valine/IleRS was 26. The stability of IleRS was checked by monitoring the aminoacylation activity. No loss of the aminoacylation activity was found, within experimental error (6%), in the course of sample preparation and NMR measurements for 24 h at 37 °C.

The 400-MHz proton NMR spectra, with 16K data points for the spectral width of 5.0 kHz, were recorded on Bruker AM-400 and WM-400 spectrometers. The measurements were carried out at a probe temperature of 37 °C. A total of 200–300 transients were accumulated, and a line broadening of 1 Hz was applied. Chemical shifts were measured relative to the methyl proton resonance of internal 2,2-dimethyl-2-silapentane-5-sulfonate. The peak intensities of the proton resonances of amino acid (L-isoleucine or L-valine) in the presence of IleRS were obtained from the difference between the proton NMR spectrum of the mixture of amino acid and IleRS and that of IleRS alone.

For each of the proton resonances of amino acid, the TRNOE action spectrum [the dependence of the resonance intensity on the frequency of irradiation (40 dB below 0.2 W) at the interval of 0.02–0.1 ppm] was obtained with selective irradiation for a constant time, prior to the acquisition of the free induction decay (1.6 s). The sum of the delay (prior to irradiation) and the duration of irradiation was set as 1.0 s, so that the recovery of proton magnetization of amino acid (and IleRS) was kept constant. The effect of spin diffusion (from the protein globule of IleRS to the ligand amino acid) was approximately eliminated by taking $I(t)/I_c(t)$, where $I_c(t)$ is the intensity of the ligand resonance on a control irradiation (at 4.3 ppm) of the protein globule (Clore & Gronenborn, 1983).

In the measurements of the time-dependent TRNOE on the proton resonances of ligand amino acid, each nonexchangeable proton of the free molecule was selectively irradiated (36 dB below 0.2 W) for up to 0.8 s in a series of experiments, prior to the acquisition of free induction decay (1.6 s). The sum of the delay (prior to irradiation) and the duration of irradiation was again set as 1.0 s. Thus, the resonance intensity of ligand amino acid, $I(t)$, was measured as a function of the duration (t) of irradiation. The effect of spin diffusion was approximately eliminated as described above.

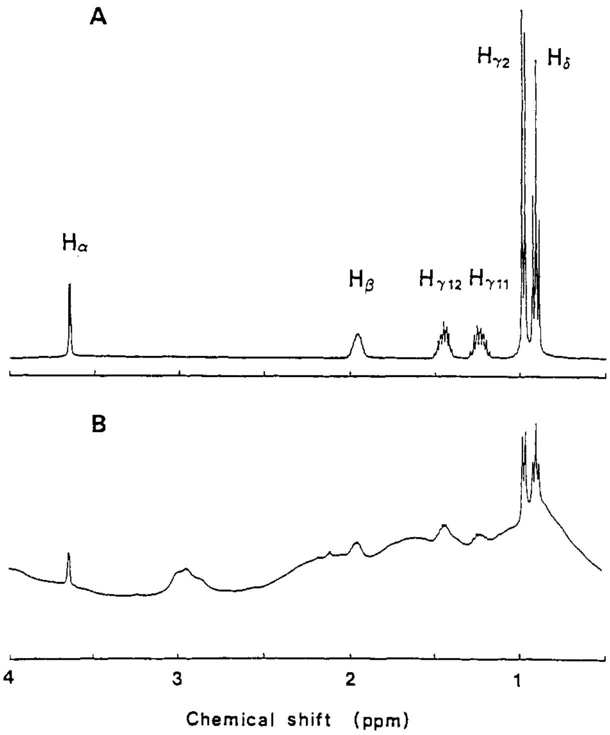

FIGURE 1: 400-MHz proton NMR spectra of (A) L-isoleucine (10 mM) and (B) L-isoleucine (4.8 mM) in the presence of *E. coli* IleRS (0.30 mM) in ^2H_2O solution (37 °C, pH 7.0) containing 10 mM potassium phosphate and 50 mM KCl. The nomenclature for L-isoleucine (IUPAC–IUB CBN, 1970) is shown in Figure 6.

RESULTS AND DISCUSSION

Proton NMR Spectra of L-*Isoleucine and* L-*Valine in the Presence of IleRS.* The 400-MHz proton NMR spectra of free L-isoleucine and L-valine are shown in Figures 1A and 2A, respectively, where the resonance assignments of the γ1-methylene group of L-isoleucine (Crout et al., 1980) and the γ-methyl groups of γl-valine (Hill et al., 1973; Aberhart & Lin, 1973) have been established. The NMR spectra of L-isoleucine (4.8 mM) or L-valine (7.9 mM) in the presence of *E. coli* IleRS (0.3 mM) are shown in Figures 1B and 2B, respectively. For the complexes of L-isoleucine–IleRS and L-valine–IleRS, the dissociation constants were determined to be 0.010 and 0.73 mM, respectively, from the fluorescence analyses of IleRS-bound TNS in the presence of amino acid (data not shown). Thus, in the solutions for NMR measurements, 99.8% of IleRS forms a complex with L-isoleucine while 92% of IleRS forms a complex with L-valine. The proton resonances of L-isoleucine and L-valine are remarkably broader in the presence of IleRS than in the absence of IleRS (Figures 1 and 2), because of the chemical exchange with the IleRS-bound molecules.

The proton resonances of L-isoleucine in the presence of IleRS were significantly broadened as the temperature was raised from 30 to 50 °C (data not shown). This indicates that the chemical exchange of L-isoleucine between the free state and the IleRS-bound state at 37 °C is slow on the NMR chemical shift scale. In fact, as shown in Figure 1B, the prominent proton resonances of the free L-isoleucine (93.7%) were observed separately from the proton resonances of the complex of L-isoleucine (6.3%) and IleRS which are very

---

[2] Direct pH meter reading not corrected for the isotope effect.

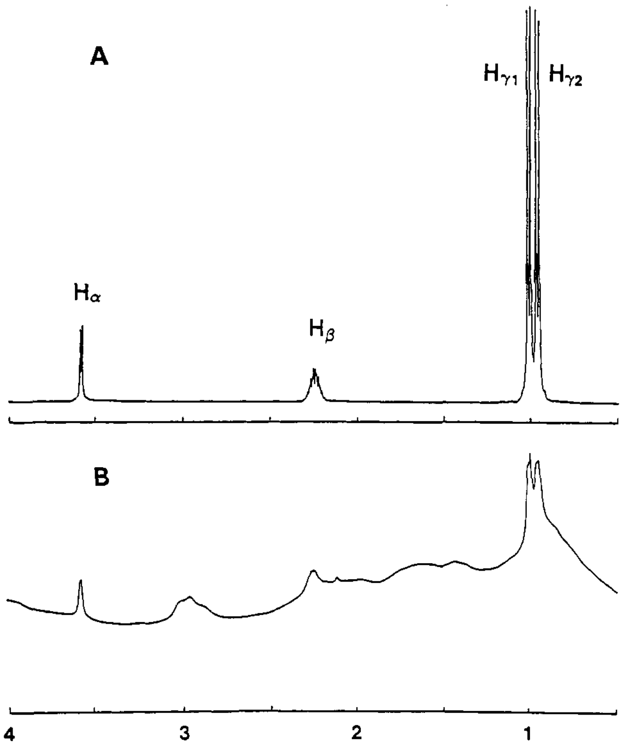

FIGURE 2: 400-MHz proton NMR spectra of (A) L-valine (10 mM) and (B) L-valine (7.9 mM) in the presence of *E. coli* Ile*RS* (0.30 mM) in ^2H_2O solution (37 °C, pH 7.0) containing 10 mM potassium phosphate and 50 mM KCl. The nomenclature for L-valine (IUPAC-IUB CBN, 1970) is shown in Figure 6.

broad. This slow exchange of L-isoleucine between the free state and bound state is consistent with the slow dissociation rate (15 s^{-1}) of the L-isoleucine–IleRS complex (Holler & Calvin, 1972).

However, the proton resonances of L-valine in the presence of IleRS (Figure 2B) were appreciably broader than those of L-isoleucine in the presence of IleRS (Figure 1B). Those proton resonances of L-valine were only slightly broadened as the temperature was raised from 30 to 40 °C, and some of those resonances became sharper again as the temperature was further raised up to 50 °C (data not shown). This indicates that the exchange rates of L-valine between the free state and the IleRS-bound state are rather fast on the chemical shift scale, and appreciably faster than those of L-isoleucine at 37 °C. Thus, the observed proton resonances of L-valine (Figure 2B) are the hybrid resonances of the free molecule (96.5%) and the IleRS-bound molecule (3.5%). In fact, the dissociation constant of the L-valine–IleRS complex is 70 times as large as that of the L-isoleucine–IleRS complex, and the dissociation rate of the L-valine–IleRS complex is probably much faster than 15 s^{-1}.

TRNOE of L-*Isoleucine in the Presence of IleRS.* The relative resonance intensity, $I(t)/I_c(t)$ of the H_α proton on irradiation (duration of 0.6 s) of the H_β proton of L-isoleucine (4.8 mM) was measured. In the presence of IleRS (0.3 mM), the resonance intensity change of −16% was observed, in contrast to the negligible NOE (0%) for L-isoleucine in the absence of IleRS. Therefore, this significant NOE (−16%) is due to the exchange of the L-isoleucine molecule between the free state and the IleRS-bound state (TRNOE).

On addition of ATP·Mg (4.8 mM), this TRNOE was remarkably decreased to −2%, becoming nearly equal to the NOE (0%) for L-isoleucine in the absence of IleRS. Isoleucyl adenylate, as formed from L-isoleucine and ATP·Mg by IleRS, is known to bind to the amino acid activation site of IleRS much more tightly than L-isoleucine, where the dissociation constant of isoleucyl adenylate–IleRS has been estimated to be as small as about 10 nM (Holler & Calvin, 1972; Holler et al., 1973). These indicate that the TRNOE of L-isoleucine in the presence of IleRS is due to the interproton cross-relaxation of L-isoleucine in the amino acid activation site of IleRS.

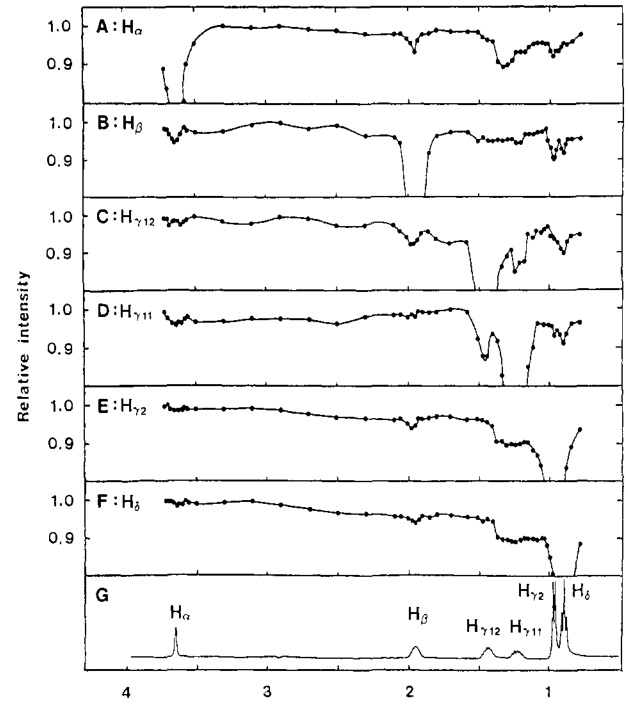

FIGURE 3: TRNOE action spectra of (A) H_α, (B) H_β, (C) $H_{\gamma 12}$, (D) $H_{\gamma 11}$, (E) $H_{\gamma 2}$, and (F) H_δ protons of L-isoleucine (5.1 mM) in the presence of IleRS (0.32 mM) at 37 °C, where the relative peak intensities of the proton resonances of L-isoleucine in the presence of IleRS were obtained from the difference between the proton NMR spectrum of the mixture of L-isoleucine and IleRS and that of IleRS alone. The duration of irradiation was set at 0.3 s. The proton NMR spectrum of L-isoleucine in the presence of IleRS, from which the spectrum of IleRS alone has been subtracted, is shown (G) for comparison.

TRNOE of L-*Valine in the Presence of IleRS.* For L-valine (7.9 mM) in the presence of IleRS (0.3 mM), a remarkable intensity change of −34% (TRNOE) was observed for the H_α proton resonance on irradiation of the H_β proton (duration of 0.6 s), in contrast to the negligible NOE (0%) of L-valine in the absence of IleRS. However, on simultaneous addition of ATP·Mg (3.9 mM) and L-isoleucine (3.9 mM) to the system of L-valine and IleRS, the TRNOE of L-valine was decreased to 0%, because of the tight binding of isoleucyl adenylate to IleRS. These indicate that the TRNOE of L-valine in the presence of IleRS is also primarily due to the interproton cross-relaxation of L-valine in the amino acid activation site of IleRS.

TRNOE Action Spectra. The TRNOE action spectra of L-isoleucine in the presence of IleRS are shown in Figure 3. At the chemical shifts of proton resonances of the free L-isoleucine, relative intensity minima due to intramolecular TRNOEs were observed. These will be discussed in detail in the analyses of the conformations of L-isoleucine as bound to IleRS.

Other than these intramolecular TRNOE minima, some broad minima were observed in the TRNOE action spectra, not corresponding to any proton resonances of free L-isoleucine. For example, in both of the action spectra for γ2-methyl

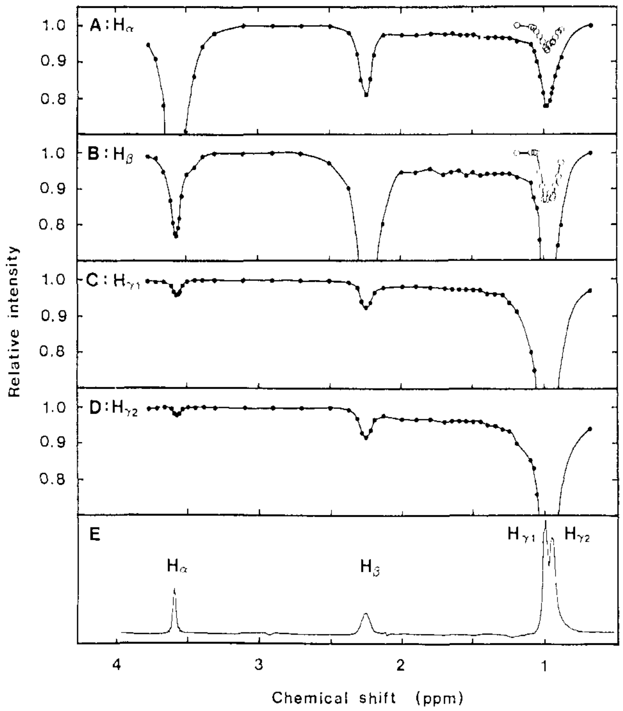

FIGURE 4: TRNOE action spectra of (A) H_α, (B) H_β, (C) $H_{\gamma1}$, and (D) $H_{\gamma2}$ protons of L-valine (7.6 mM) in the presence of IleRS (0.29 mM) at 37 °C, where the relative peak intensities of the proton resonances of L-valine were obtained from the difference between the proton NMR spectrum of the mixture of L-valine and IleRS and that of IleRS alone. The duration of irradiation was set at 0.15 s (○) or 0.60 s (●). The proton NMR spectrum of L-valine in the presence of IleRS, from which the spectrum of IleRS alone has been subtracted, is shown (E) for comparison.

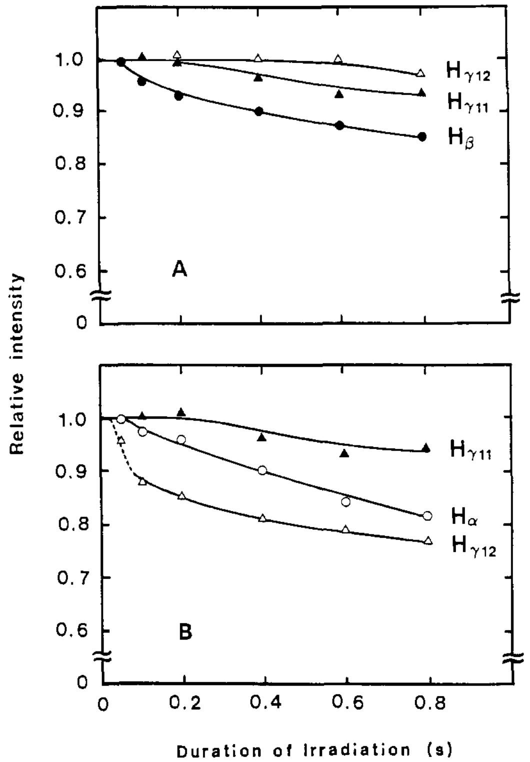

FIGURE 5: Dependence, on irradiation time, of the relative resonance intensities $[I(t)/I_c(t)]$ of the H_α (○), H_β (●), $H_{\gamma12}$ (△), and $H_{\gamma11}$ (▲) protons on irradiation of the H_α (A) and H_β (B) protons of L-isoleucine (4.9 mM) in the presence of Ile RS (0.31 mM) at 37 °C. The relative intensities of proton resonances were obtained as described in the legend of Figure 3. As for the relative intensity of the $H_{\gamma12}$ proton on irradiation of the H_β proton, the profile is composed of a fast process (dashed line) and a slow process (solid line) (see text).

protons (Figure 3E) and for δ-methyl protons (Figure 3F) of L-isoleucine, broad minima were clearly observed at 1.35 ppm. These minima possibly arise from (1) saturation transfer of the ligand protons from the IleRS-bound state to the free state, (2) intramolecular TRNOE by irradiation of other ligand protons in the IleRS-bound state, and/or (3) TRNOE by irradiation of IleRS protons in close proximity to the ligand protons in the bound state (intermolecular TRNOE).

On the other hand, in the action spectrum for the H_α proton of L-isoleucine (Figure 3A), the broad minimum at 1.35 ppm is far from the H_α proton resonance of free L-isoleucine (3.64 ppm). This minimum is probably due to the intermolecular TRNOE by irradiation of methyl or methylene proton(s) of IleRS. In the action spectrum for the $H_{\gamma12}$ proton (Figure 3C), similar broad minima were observed at 1.7 and 2.0 ppm (close to the H_β proton resonance of free L-isoleucine). However, the minimum at 1.7 ppm was not observed in the action spectra for any other proton resonances of free L-isoleucine (Figure 3). Accordingly, one or both of these minima at 2.0 and 1.7 ppm (Figure 3C) are probably due to the intermolecular TRNOE by irradiation of protons of IleRS.

TRNOE action spectra of L-valine in the presence of IleRS are shown in Figure 4. Because the exchange rate of L-valine between the free state and the IleRS-bound state is intermediate on the chemical shift scale, the hybrid proton resonances of L-valine in these two states were observed (Figures 2 and 4). At the chemical shifts of these hybrid proton resonances of L-valine, relative intensity minima due to intramolecular TRNOEs were observed. In addition, broad minima at 2–1 ppm were observed because of intermolecular TRNOEs.

Time-Dependent TRNOE. In the present study on the conformations of L-isoleucine and L-valine bound to IleRS, the dependences of relative resonance intensities of ligand protons on the duration of selective irradiation of another ligand proton were measured. In such measurements, the decoupler power level was set appreciably higher than that in the measurements of TRNOE action spectra, and thus the resonances of irradiated protons were saturated within the short duration before the acquisition of free induction decay (Clore & Gronenborn, 1983). If the rates of exchange between the free state and the IleRS-bound state are fast as compared with the cross-relaxation rates in the bound state, the cross-relaxation rate (σ), for the pair of the irradiated proton and the observed proton, may be approximately estimated from $\sigma = S_i/b$, where S_i is the initial slope $-d[I(t)/I_c(t)]/dt$ at $t = 0$ and b is the mole fraction of ligand in the bound state (Clore & Gronenborn, 1983).

However, in all the time-dependent TRNOE profiles for the proton pairs of the free L-isoleucine in the presence of IleRS (Figure 5), there are lag phases prior to the time-dependent decrease in the relative intensities of the observed proton resonances. These lag phases were of about 0.03 s for the pair H_β–$H_{\gamma12}$, of about 0.05 s for the pair H_α–H_β, and even longer for the pairs H_α–$H_{\gamma12}$, H_α–$H_{\gamma11}$, and H_β–$H_{\gamma11}$. Since the decoupler power level is set high enough, the lag phases of 0.03–0.05 s are probably due to the rates of exchange between the free state and the IleRS-bound state which are not fast as compared with the cross-relaxation rates in the bound state. In fact, the dissociation rate of the L-isoleucine–IleRS complex (15 s^{-1}; Holler & Calvin, 1972) is possibly of the same order of magnitude as the proton cross-relaxation rates of L-isoleucine in the IleRS-bound state.

Simulation of the Time-Dependent TRNOE in the Intermediate Exchange Condition. Under such conditions, time-dependent TRNOE profiles for a system of two protons of a

Table I: Apparent Cross-Relaxation Rates (and Standard Deviations) (σ', s^{-1})[a] of IleRS-Bound L-Isoleucine at 37 °C and Inverse Sixth Power of Interproton Distances (r^{-3}, 10^3 nm^{-6})[b] for Rotamers of L-Isoleucine

			r^{-6}, rotamer about $N-C_\alpha-C_\beta-C_{\gamma 1}$[c]		
H1 (irr)	H2 (obsd)	σ'	gauche$^+$	gauche$^-$	trans
H_α	H_β	7 ± 3	0.41	0.11	0.41
H_β	H_α	6 ± 2			
H_α	$H_{\gamma 12}$	*d*	0.04	0.11	0.41
$H_{\gamma 12}$	H_α	*d*			
H_α	$H_{\gamma 11}$	*d*	0.04	0.41	0.11
$H_{\gamma 11}$	H_α	*d*			

			r^{-6}, rotamer about $C_\alpha-C_\beta-C_{\gamma 1}-C_\delta$		
H1 (irr)	H2 (obsd)	σ'	gauche$^+$	gauche$^-$	trans
H_β	$H_{\gamma 12}$	6 ± 3	0.11	0.41	0.41
H_β	$H_{\gamma 11}$	*d*	0.41	0.41	0.11

[a] On irradiation of proton H1, the resonance of proton H2 is observed. [b] Distances between proton H1 and proton H2. [c] In the case of the trans form about $C_\alpha-C_\beta-C_{\gamma 1}-C_\delta$. [d] σ' is 0–2 s^{-1} after a spin-diffusion lag phase for as long as 0.2 s was observed.

Table II: Apparent Cross-Relaxation Rates (and Standard Deviations) (σ', s^{-1})[a] of IleRS-Bound L-Valine at 37 °C and (Averaged) Inverse Sixth Power of Interproton Distances (r^{-6}, 10^3 nm^{-6})[b] for Rotamers about $N-C_\alpha-C_\beta-C_{\gamma 1}$ of L-Valine

			r^{-6}		
H1 (irr)	H2 (obsd)	σ'	gauche$^+$	gauche$^-$	trans
H_α	H_β	24 ± 3	0.41	0.41	0.11
H_β	H_α	16 ± 2			

			$(r_1^{-6} + r_2^{-6} + r_3^{-6})/3$[c]		
H1 (irr)	H2 (obsd)	σ'	gauche$^+$	gauche$^-$	trans
H_α	$H_{\gamma 1}$	4 ± 2	0.03	0.19	0.19
H_α	$H_{\gamma 2}$	*d*	0.19	0.03	0.19
H_β	$H_{\gamma 1}$	7 ± 2	0.31	0.31	0.31
H_β	$H_{\gamma 2}$	9 ± 2	0.31	0.31	0.31

[a] On irradiation of proton H1, the resonance of proton H2 is observed. [b] Distances between proton H1 and proton H2. [c] r_i ($i = 1-3$) is the distance between a non-methyl proton and the *i*th proton of a methyl group. [d] σ' is 0–2 s^{-1}, after a spin-diffusion lag phase for as long as 0.2 s was observed.

ligand were simulated (see the Appendix). For example, take the cross-relaxation rate in the IleRS-bound state as $\sigma = 15$ s^{-1} and the dissociation rate as 15 s^{-1}. Then, for the relative resonance intensity of the observed proton of the *free* ligand, a short lag phase ("exchange lag phase") of about 0.05 s certainly appears after irradiation of the other ligand proton, and then the resonance intensity of the observed proton is decreased (see solid lines in Figure 7). The "apparent initial slope" (S'_i) in this case of intermediate dissociation rate is as small as about 25% of the initial slope S_i ($=b\sigma$) in the case of fast dissociation rate (600 s^{-1}, see dashed lines in Figure 7). Further, for a series of simulated profiles (with fixed values of dissociation rate and spin–lattice relaxation rates), the S'_i values are approximately proportional to the cross-relaxation rates (σ) for the pair of two protons (solid lines in Figure 7, Appendix). Therefore, even for L-isoleucine in the presence of IleRS, the observed values of S'_i/b (apparent cross-relaxation rate, σ') may be assumed to be proportional to the cross-relaxation rates for L-isoleucine in the IleRS-bound state.

Apparent Cross-Relaxation Rates of IleRS-Bound L-Isoleucine. As for L-isoleucine (4.9 mM) in the presence of IleRS (0.31 mM), the dependence of $I(t)/I_c(t)$ on time t (the duration of irradiation) is shown in Figure 5A. On irradiation of the H_α proton, the resonance intensity of the H_β proton was significantly decreased with time, even for t as short as 0.1 s. With an exchange lag phase for 0.05 s, the apparent initial slope S'_i was obtained. From this value of S'_i and the mole fraction ($b = 0.063$) of IleRS-bound L-isoleucine, the apparent cross-relaxation rate (σ') was estimated as 7 (±3) s^{-1} (Table I). Conversely, on irradiation of the H_β proton (Figure 5B), the resonance intensity of the H_α proton was also decreased with t, and the apparent cross-relaxation rate (σ') was obtained as 6 (±2) s^{-1}.

As for the $H_{\gamma 12}$ proton of L-isoleucine in the presence of IleRS, the resonance intensity was decreased significantly on irradiation of the H_β proton even within 0.05 s of duration, where the exchange lag phase appears to be as short as about 0.03 s. Subsequently, the resonance intensity of this proton was gradually decreased as the duration was increased up to 0.8 s (Figure 5B). In comparison, in the action spectrum for this $H_{\gamma 12}$ proton (Figure 3C, irradiation for 0.3 s), there is a broad minimum at 2.0 ppm probably due to the intermolecular TRNOE between L-isoleucine and IleRS, in addition to a sharp minimum at 1.96 ppm due to the specific intramolecular TRNOE between $H_{\gamma 12}$ and H_β. The broad minimum at 2.0 ppm, rather than the sharp minimum at 1.96 ppm, was also observed in an action spectrum with irradiation for as short as 0.05 s (data not shown). Therefore, in the time-dependent TRNOE of the $H_{\gamma 12}$ proton by the irradiation of H_β proton (Figure 5B), the initial intensity decrease (within the duration t for 0.05 s) is primarily due to the intermolecular TRNOE, and the following decrease (for $t > 0.05$ s) is due to the intramolecular TRNOE. Further, the exchange lag phase for the intermolecular TRNOE is, in fact, expected to be as short as about half of that for the intramolecular TRNOE in the intermediate exchange condition (Appendix). From the apparent slope (S'_i) for this intramolecular TRNOE and the mole fraction ($b = 0.063$) of IleRS-bound L-isoleucine, the cross-relaxation rate σ' for the pair of H_β proton and $H_{\gamma 12}$ proton was obtained as 6 (±3) s^{-1} (Table I).

Spin Diffusion Lag Phase. By contrast, the resonance intensity of the $H_{\gamma 12}$ or $H_{\gamma 11}$ proton was not decreased with the duration $t < 0.2$ s of irradiation of the H_α proton (Figure 5A). Conversely, for the resonance intensity of the H_α proton on irradiation of the $H_{\gamma 12}$ or $H_{\gamma 11}$ proton, a lag phase for $t < 0.2$ s was also observed (Table I). Similarly, a lag phase for about 0.2 s was observed for the resonance intensity of the $H_{\gamma 11}$ proton on irradiation of the H_β proton (Figure 5B). This lag phase for about 0.2 s is much longer than the exchange lag phase for 0.05 s due to the intermediate exchange rates (Appendix). Consequently, the decrease in the resonance intensity after such a lag phase for as long as 0.2 s is probably due to the spin diffusion through other protons of L-isoleucine and/or protons of IleRS ("spin-diffusion lag phase") (Clore & Gronenborn, 1983). Thus, for the proton pairs $H_\alpha-H_{\gamma 12}$, $H_\alpha-H_{\gamma 11}$, and $H_\beta-H_{\gamma 11}$, the direct cross-relaxation rate is particularly slow (slower than 2 s^{-1}, the mean value of standard deviation for the apparent cross-relaxation rate).

Apparent Cross-Relaxation Rates of IleRS-Bound L-Valine. In the case of L-valine, as described above, the rates of exchange between the free state and the IleRS-bound state are probably fast as compared with the cross-relaxation rates, and also fast on the chemical shift scale. Under such conditions, exchange lag phases are expected to be very short (see the Appendix). In fact, as for the proton resonances of L-valine (8.6 mM) in the presence of IleRS (0.33 mM), there was no indication of exchange lag phases on irradiation of the α-proton or β-proton (data not shown). Therefore, from the initial slopes (S'_i) and the mole fraction ($b = 0.035$) of IleRS-bound L-valine, the apparent cross-relaxation rates (σ') for proton pairs

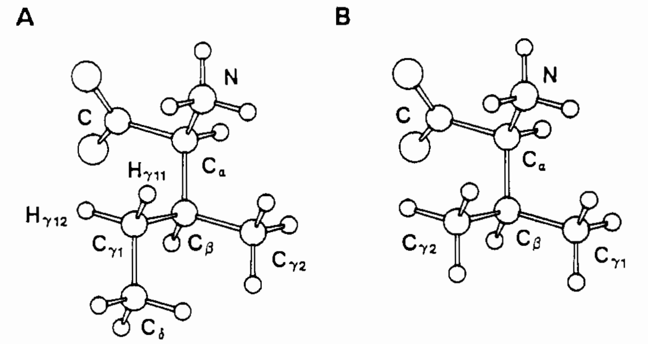

FIGURE 6: Conformations of (A) L-isoleucine and (B) L-valine as bound in the amino acid activation site of *E. coli* isoleucyl-tRNA synthetase.

were obtained as shown in Table II. Because of the fast exchange, these apparent cross-relaxation rates (σ') are actually equal to the cross-relaxation rates (σ) for proton pairs of IleRS-bound L-valine. For the resonance intensity of the H_α proton on irradiation of $H_{\gamma 2}$ methyl protons, a spin-diffusion lag phase was observed (Table II).

Conformation of IleRS-Bound L-*Isoleucine.* As the L-isoleucine molecule is tightly bound to the active site of IleRS, the correlation time for the interproton dipole interaction may be assumed to be common for any pairs of protons (not involving methyl protons) of L-isoleucine in the IleRS-bound state. Thus, the apparent cross-relaxation rates for this system may well be treated as being approximately proportional to the inverse sixth power of interproton distances.

The apparent cross-relaxation rate (σ') for the pair H_β–$H_{\gamma 12}$ was obtained as 6 ± 3 s^{-1} (Table I). By contrast, for the pair H_β–$H_{\gamma 11}$, a spin-diffusion lag phase was observed (Table I), indicating that σ' is negligibly slow. Clearly, the H_β proton is closer to the $H_{\gamma 12}$ proton than to the $H_{\gamma 11}$ proton. In comparison, the inverse sixth power of interproton distances (r^{-6}) was calculated for the three possible rotamers (gauche$^+$, gauche$^-$, and trans forms) about the C_α–C_β–$C_{\gamma 1}$–C_δ skeleton (Table I). Only in the trans form is r^{-6} much larger for the pair H_β–$H_{\gamma 12}$ than for the pair H_β–$H_{\gamma 11}$. Accordingly, in the IleRS-bound L-isoleucine, the C_α–C_β–$C_{\gamma 1}$–C_δ skeleton is now found to take the trans form as shown in Figure 6A.

As for the conformation about the N–C_α–C_β–$C_{\gamma 1}$ skeleton of IleRS-bound L-isoleucine, the apparent cross-relaxation rates (σ') for the pairs involving the H_α proton (Table I) indicate that the H_α proton is much closer to the H_β proton than to the $H_{\gamma 12}$ and $H_{\gamma 11}$ protons. These cross-relaxation rates were compared with the inverse sixth power of interproton distances (r^{-6}) in the three possible rotamers about the N–C_α–C_β–$C_{\gamma 1}$ skeleton, where the C_α–C_β–$C_{\gamma 1}$–C_δ skeleton is set in the trans form (Table I). Only in the gauche$^+$ form about the N–C_α–C_β–$C_{\gamma 1}$ skeleton is r^{-6} for the pair H_α–H_β much larger than those for the pairs H_α–$H_{\gamma 12}$ and H_α–$H_{\gamma 11}$. Accordingly, in the IleRS-bound L-isoleucine, the N–C_α–C_β–$C_{\gamma 1}$ skeleton is found to take the gauche$^+$ form (Figure 6A).

TRNOEs for Pairs of Methyl Protons and Non-Methyl Protons. The cross-relaxation processes among protons including methyl protons are more complicated than those among non-methyl protons only (Tropp, 1980; Inagaki et al., 1982). Cross-relaxation rates for pairs of non-methyl protons and methyl protons are expected to be lower than those for pairs of non-methyl protons, even if the interproton distances are the same. This is because of the fast internal rotation of the methyl group as compared with the overall rotation of the L-isoleucine–IleRS complex. Further, in such "methyl–non-methyl" cases, cross-relaxation rates depend, for example, on the angle between the interproton vector and the internal rotation axis of the methyl group (Tropp, 1980; Inagaki et al., 1982). Nevertheless, the methyl–non-methyl cross-relaxation rates are nearly proportional to the average values of the inverse sixth power of the interproton distances, $(r_1^{-6} + r_2^{-6} + r_3^{-6})/3$ where r_i (i = 1–3) is the distance between a non-methyl proton and the ith proton of a methyl group. Accordingly, the methyl–non-methyl TRNOEs are still useful for comparison of the proximity among protons involved.

Practically in the methyl proton region of the action spectra for non-methyl proton resonances, the signal-to-noise ratios are high enough, probably because of simultaneous irradiation of the three protons of each methyl group. On the basis of such action spectra, the conformation of IleRS-bound L-isoleucine (Figure 6A) was confirmed. In the TRNOE action spectra both for the H_β proton (Figure 3B) and for the $H_{\gamma 11}$ proton (Figure 3D), two minima (0.98 and 0.91 ppm) were observed in the 1.1–0.8 ppm region, corresponding to the γ2- and δ-methyl proton resonances. By contrast, in the TRNOE action spectrum for the H_α proton, only one minimum (0.98 ppm) was observed in this region, corresponding to the γ2-methyl proton resonance (Figure 3A). Similarly, only one minimum (0.91 ppm, corresponding to the δ-methyl group) was observed in the TRNOE action spectrum for the $H_{\gamma 12}$ proton (Figure 3C). Consequently, these TRNOE action spectra confirm the predominance of the conformer of IleRS-bound L-isoleucine (Figure 6A), although the possibility of the minor presence of other conformers may not be discarded.

Conformation of IleRS-Bound L-*Valine.* The conformation of L-valine in the IleRS-bound state (Figure 6B) may now be discussed on the basis of time-dependent TRNOEs and TRNOE action spectra involving methyl protons. On irradiation of the H_β proton, the apparent cross-relaxation rates (σ') for the γ1-methyl proton and for the γ2-methyl proton were found to be much the same (Table II), just as expected from the geometry around the C_β atom (Figure 6B). On the other hand, the apparent cross-relaxation rate σ' for the proton pair H_α–$H_{\gamma 1}$ is much higher than that for the proton pair H_α–$H_{\gamma 2}$. In comparison, for each of the three rotamers about the C_α–C_β bond of L-valine, the average values of inverse sixth power of the distances between a non-methyl proton (H_α or H_β) and the three protons of a methyl group ($H_{\gamma 1}$ or $H_{\gamma 2}$) were obtained, as shown in Table II. The cross-relaxation rates as observed in methyl–non-methyl TRNOE are expected to be nearly proportional to the average values of r^{-6}, since the relative geometry of the non-methyl proton and the methyl group is rather similar among the three rotamers about the C_α–C_β bond (Tropp, 1980; Inagaki et al., 1982). Only for the gauche$^-$ form about the N–C_α–C_β–$C_{\gamma 1}$ skeleton, the order of the average values of r^{-6} agrees with the order of the observed values of σ' (Table II). Thus, the N–C_α–C_β–$C_{\gamma 1}$ skeleton of L-valine is clearly found to take the gauche$^-$ form in the IleRS-bound state (Figure 6B).

The effects of irradiation of the methyl protons on the H_α and H_β proton resonances of L-valine were observed in action spectra (Figure 4A,B), since the proton resonances of these methyl groups are in close proximity to each other (Figure 2B). For the H_β proton, two minima (1.00 and 0.96 ppm) were observed in the 1.1–0.8 ppm region, corresponding to the γ1-methyl and γ2-methyl proton resonances, respectively (Figure 4B). By contrast, for the H_α proton (Figure 4A), only one minimum (1.00 ppm), corresponding to the γ1-methyl proton resonance, was observed in the 1.1–0.8 ppm region. These confirm the predominance of the conformation of the IleRS-bound L-valine as shown in Figure 6B.

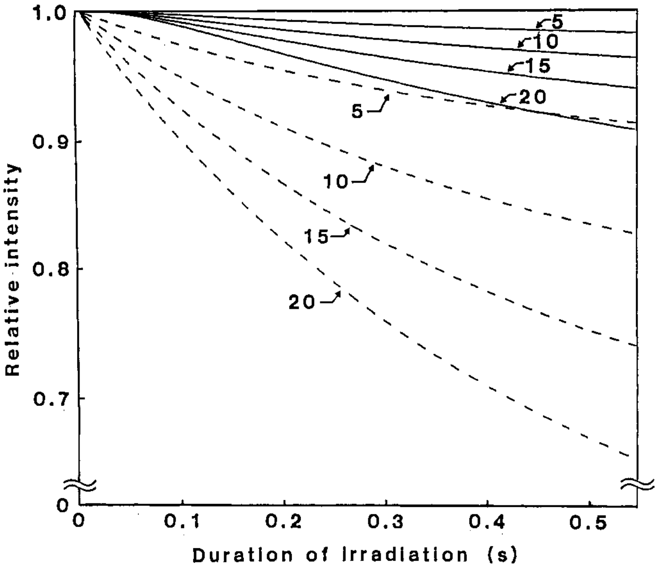

FIGURE 7: Simulation of the dependence of the relative resonance intensity of proton 1 (M_{1F}/M_{0F}) on the duration of irradiation of proton 2, in the relatively slow exchange condition ($k_- = 15\ \mathrm{s}^{-1}$, solid lines) and in the fast exchange condition ($k_- = 600\ \mathrm{s}^{-1}$, dashed lines), for a variety of cross-relaxation rates (σ_B = 5, 10, 15, or 20 s^{-1} as indicated in the figure). Other parameters used in the simulation are $b = 0.063$, $\rho_{1B} = \rho_{2B} = 23\ \mathrm{s}^{-1}$, $\rho_{1F} = 1\ \mathrm{s}^{-1}$, and $\sigma_F = 0$.

Finally, the apparent cross-relaxation rate of IleRS-bound L-valine may be compared with that of IleRS-bound L-isoleucine. Thus, for the pair of H_α and H_β protons of L-valine, the apparent cross-relaxation rate σ' was obtained as about 20 s^{-1} (Table II), which was significantly faster than that (6 s^{-1}) of IleRS-bound L-isoleucine (Table I). However, the interproton distance for the pair H_α–H_β in L-valine is expected to be equal to that in L-isoleucine, since the conformations about the C_α–C_β bond of the two molecules are found to be the same as each other (Figure 6). Therefore, the difference in the apparent cross-relaxation rates between L-isoleucine and L-valine in the presence of IleRS is consistent with the difference in the dissociation rates between the L-isoleucine–IleRS complex and the L-valine–IleRS complex.

Recognition of L-*Isoleucine and* L-*Valine by IleRS.* IleRS is known to recognize the amino group and the carboxyl group of amino acids, since the modifications of these groups of L-isoleucine reduce the affinity with IleRS (Holler et al., 1973). The spatial arrangements (relative to the amino group and the carboxyl group) of the side chains of L-isoleucine and L-valine in the IleRS-bound molecules are shown in Figure 6. Thus, in the IleRS-bound state, these molecules take the same conformation except for the δ-methyl group of L-isoleucine. Accordingly, the side chain of L-valine will occupy the pocket in the activation site of IleRS for L-isoleucine, leaving vacant space provided for the δ-methyl group of L-isoleucine.

The modes of the interaction of IleRS with L-isoleucine and L-valine will be discussed on the basis of the intermolecular TRNOEs. In the TRNOE action spectra for the H_α and $H_{\gamma 12}$ protons (and also for the $H_{\gamma 2}$ and H_δ protons) of L-isoleucine (Figure 3), broad but significant minima were observed in the aliphatic proton region. This suggests that the side chain of L-isoleucine lies in a hydrophobic pocket provided by aliphatic amino acid residues of the active site on IleRS. Further, the hydrophobic interaction of L-isoleucine with the active site of IleRS appears to be more significant than that of L-valine, since remarkable intermolecular TRNOE was observed for the system of IleRS and L-isoleucine (Figure 3) rather than for the system of IleRS and L-valine (Figure 4). This is consistent with the finding, from the TNS fluorescence analyses, that the binding constant of L-valine to the amino acid activation site of IleRS is about 2% of that of L-isoleucine (Holler et al., 1973; present study).

The present study has demonstrated that the molecular conformation of amino acid bound to aminoacyl-tRNA synthetase may be elucidated by the analysis of TRNOE. This method will also be useful for the conformation analyses of amino acid analogues, which would provide detailed information on the molecular mechanism of strict recognition of aminoacyl-tRNA synthetases. Thus, the conformational analyses of a series of isoleucine analogues, including L-alloisoleucine and furanomycin, are now in progress in our laboratory.

Acknowledgments

We are grateful to Dr. Fuyuhiko Inagaki (Tokyo Metropolitan Institute of Medical Science) for discussion and to Bruker Japan for the use of the Bruker WM-400 spectrometer.

Appendix

Simulation of Time-Dependent TRNOE. For a ligand in equilibrium between the free state and enzyme-bound state, the dependence of the resonance intensity of the proton on the duration of irradiation of another proton will be discussed here. As for the averaged proton resonances in the case that the exchange rate between the free state and bound state is fast on the chemical shift scale and also fast as compared with the cross-relaxation rates of the protons in the bound state, the time-dependent TRNOE profiles have already been simulated (Clore & Gronenborn, 1983). Here, in the case that the exchange rate is slow on the chemical shift scale, the time-dependent TRNOE profiles are simulated for the proton resonances of the free ligand. The scheme of the equilibrium is

$$\mathrm{E} + \mathrm{L} \underset{k_-}{\overset{k_+}{\rightleftharpoons}} \mathrm{EL}$$

where E, L, and EL are the free enzyme, the free ligand, and the ligand–enzyme complex, respectively. In a simple case of ligand with two protons, the modified Bloch equations for protons i (i = 1, 2) and j ($j \neq i$) are given by

$$\mathrm{d}M_{iB}/\mathrm{d}t = -\rho_{iB}(M_{iB} - M_{0B}) + \sigma_B(M_{jB} - M_{0B}) - k_- M_{iB} + k_+[\mathrm{E}]M_{iF}$$

$$\mathrm{d}M_{iF}/\mathrm{d}t = -\rho_{iF}(M_{iF} - M_{0F}) + \sigma_F(M_{jF} - M_{0F}) + k_- M_{iB} - k_+[\mathrm{E}]M_{iF}$$

where the suffixes B and F denote the bound state and the free state, respectively, of the ligand, M_{iB} and M_{iF} are the magnetizations (z components) of proton i, M_{0B} and M_{0F} are the equilibrium magnetizations, ρ_{iB} and ρ_{iF} are the longitudinal relaxation rates, and σ_B and σ_F are the cross-relaxation rates (σ_B is positive and σ_F is negative). These equations were numerically solved on the assumption of instantaneous saturation (Dobson et al., 1982); M_{2F} was set equal to zero.

In the present study, the time-dependent TRNOE in an intermediate exchange condition ($k_- = 15\ \mathrm{s}^{-1}$, solid lines in Figure 7) was simulated for the first time, which nearly correspond to the case of L-isoleucine in the presence of IleRS. For a variety of cross-relaxation rates (σ_B = 5–20 s^{-1}), Figure 7 shows the dependence of the relative resonance intensity of proton 1 in the free state (M_{1F}/M_{0F}) on the duration of irradiation of proton 2 in the free state. In each case, a lag phase is observed before the exponential decrease in the relative intensity of proton 1. Naturally, for $t = 0$, dM_{1F}/dt is equal to 0, since M_{1B} and M_{1F} are equal to M_{0B} and M_{0F}, respectively, and $k_-M_{0B} = k_+[E]M_{0F}$. Therefore, the initial lag phase is due to the time required for the saturation transfer of the irradiated proton from the free state to the bound state and then that of the observed proton from the bound state to the free state. Accordingly, this kind of lag phase may be called an "exchange lag phase". The exchange lag phase in the case of intermediate exchange is as long as 0.05–0.06 s (solid lines in Figure 7). If, instead of the proton of the free ligand, the proton of the bound ligand or the proton of protein is irradiated, the exchange lag phase is as short as 0.02–0.03 s (data not shown), which is required for the saturation transfer of the observed proton from the bound state to the free state.

For comparison, time-dependent TRNOEs in a fast exchange condition ($k_- = 600$ s^{-1}) were simulated for the free ligand proton resonance (dashed lines in Figure 7). The exchange lag phase on the fast exchange condition is as short as 0.005 s (dashed lines), in contrast to a long lag phase (as long as 0.05–0.06 s) in the intermediate exchange condition (solid lines in Figure 7). On the other hand, on the condition that the exchange rate is fast even on the chemical shift scale, no exchange lag phase is observed for the time-dependent TRNOEs of the averaged proton resonances (Clore & Gronenborn, 1983), which corresponds probably to the case of L-valine in the presence of IleRS.

In the time-dependence profiles of relative intensity (Figure 7), the maximal slope of intensity decrease is observed just after the exchange lag phase. Such a slope may be called an "apparent initial slope" (S'_i). In the fast exchange condition ($k_- = 600$ s^{-1}), S'_i is nearly equal to $b\sigma_B$, where b is the mole fraction of the ligand in the bound state [$M_{0B}/(M_{0B} + M_{0F})$]. By contrast, even with the same value of σ_B, the apparent initial slope in the relatively slow exchange condition ($k_- = 15$ s^{-1}) is as small as about one-fourth of that in the case of the fast exchange condition (Figure 7). The apparent cross-relaxation rates ($\sigma' = S'_i/b$) are approximately proportional to the actual cross-relaxation rates (σ_B), if the longitudinal relaxation rate (ρ_{1B}) is nearly constant. Thus, even in the intermediate condition, the conformation of the bound ligand may be discussed on the basis of the time-dependent TRNOE.

If the cross-relaxation rate (σ_B) is negligibly slow, a long lag phase ("spin-diffusion lag phase") may be observed, which is followed by the intensity decrease due to spin diffusion through the indirect cross-relaxation with other protons (Clore & Gronenborn, 1983). Further, if the irradiation power is too low, the resonance saturation takes time, giving rise to "saturation lag phase" (Ferrin & Mildvan, 1985). These three types of lag phases (saturation, exchange, and spin diffusion) should be examined before the determination of the conformation of bound ligand.

Registry No. IleRS, 9030-96-0; Ile, 73-32-5; Val, 72-18-4.

REFERENCES

Aberhart, D. J., & Lin, L. J. (1973) *J. Am. Chem. Soc. 95*, 7859–7860.

Banerjee, A., Levy, H. R., Levy, G. C., & Chan, W. W.-C. (1985) *Biochemistry 24*, 1593–1598.

Cayley, P. J., Albrand, J. P., Freeney, J., Roberts, G. C. K., Piper, E. A., & Burgen, A. S. V. (1979) *Biochemistry 18*, 3886–3895.

Clore, G. M., & Gronenborn, A. M. (1983) *J. Magn. Reson. 53*, 423–442.

Clore, G. M., Gronenborn, A. M., & McLaughlin, L. W. (1984) *J. Mol. Biol. 174*, 163–173.

Crout, D. H. G., Gregorio, M. V. M., Müller, U. S., Komatsubara, S., Kisumi, M., & Chibata, I. (1980) *Eur. J. Biochem. 106*, 97–105.

Dobson, C. M., Olejniczak, E. T., Poulsen, F. M., & Ratcliffe, R. G. (1982) *J. Magn. Reson. 48*, 97–110.

Ferrin, L. J., & Mildvan, A. S. (1985) *Biochemistry 24*, 6904–6913.

Fersht, A. R. (1977) *Biochemistry 16*, 1025–1030.

Flossdorf, J., Pratorius, H.-J., & Kula, M.-R. (1976) *Eur. J. Biochem. 66*, 147–155.

Gronenborn, A. M., & Clore, G. M. (1982) *Biochemistry 21*, 4040–4048.

Gronenborn, A. M., & Clore, G. M. (1984) *J. Mol. Biol. 172*, 559–572.

Gronenborn, A. M., Clore, G. M., Hobbs, L., & Jeffery, J. (1984a) *Eur. J. Biochem. 145*, 365–371.

Gronenborn, A. M., Clore, G. M., McLaughlin, L. W., Graeser, E., Lorber, B., & Giege, R. (1984b) *Eur. J. Biochem. 145*, 359–364.

Hill, R. K., Yan, S., & Arfin, S. M. (1973) *J. Am. Chem. Soc. 95*, 7857–7859.

Holler, E., & Calvin, M. (1972) *Biochemistry 11*, 3741–3752.

Holler, E., Bennett, E. L., & Calvin, M. (1971) *Biochem. Biophys. Res. Commun. 45*, 409–415.

Holler, E., Rainey, P., Orme, A., Bennet, E. L., & Calvin, M. (1973) *Biochemistry 12*, 1150–1159.

Hopfield, J. J., Yamane, T., Yue, V., & Coutts, S. M. (1976) *Proc. Natl. Acad. Sci. U.S.A. 73*, 1164–1168.

Inagaki, F., Boyd, J., Campbell, I. D., Clayden, N. J., Hull, W. E., Tamiya, N., & Williams, R. J. P. (1982) *Eur. J. Biochem. 121*, 609–616.

IUPAC–IUB Commission on Biochemical Nomenclature (CBN) (1970) *Biochemistry 9*, 3471–3479.

Kawakami, M., Miyazaki, M., Yamada, H., & Mizushima, S. (1985) *FEBS Lett. 185*, 162–164.

Loftfield, R. B., & Eigner, E. A. (1966) *Biochim. Biophys. Acta 130*, 426–448.

Loftfield, R. B., & Vanderjagt, D. (1972) *Biochem. J. 128*, 1353–1356.

Machida, M., Yokoyama, S., Matsuzawa, H., Miyazawa, T., & Ohta, T. (1985) *J. Biol. Chem. 260*, 16143–16147.

Tropp, J. (1980) *J. Chem. Phys. 72*, 6035–6043.

Wakamatsu, K., Higashijima, T., Fujini, M., Nakajima, T., & Miyazawa, T. (1983) *FEBS Lett. 162*, 123–126.

Wakamatsu, K., Okada, A., Suzuki, M., Higashijima, T., Masui, Y., Sakakibara, S., & Miyazawa, T. (1986a) *Eur. J. Biochem. 154*, 607–615.

Wakamatsu, K., Okada, A., Higashijima, T., & Miyazawa, T. (1986b) *Biopolymers 25*, S193–S200.

Wakamatsu, K., Okada, A., Miyazawa, T., Masui, Y., Sakakibara, S., & Higashijima, T. (1987) *Eur. J. Biochem. 163*, 331–338.